Negative differential conductance and current bistability in undoped GaAs/(Al,Ga)As quantum-cascade structures

S. L. Lu, L. Schrottke, R. Hey, H. Kostial, and H. T. Grahn[a)]
Paul-Drude-Institut für Festkörperelektronik, Hausvogteiplatz 5-7, 10117 Berlin, Germany

(Received 10 August 2004; accepted 15 October 2004; published online 27 December 2004)

We have investigated negative differential conductivity (NDC) and laser level population in undoped GaAs/(Al,Ga)As quantum-cascade structures using current–voltage characteristics and interband photoluminescence spectroscopy. While for both GaAs/$Al_{0.33}Ga_{0.67}$As and GaAs/$Al_{0.45}Ga_{0.55}$As structures a strong, bistable NDC is observed, a weaker NDC without bistability appears only in the GaAs/$Al_{0.45}Ga_{0.55}$As structure, which is due to the resonant coupling between injector and upper laser level. Although the bistable NDC is connected with a significant population of the laser levels, it cannot be explained by resonant coupling between electronic states in the active region. We believe that the bistable NDC is caused by an interplay of resonant coupling effects within the injector with the carrier redistribution in the vicinity of the optically active region. Furthermore, a still unidentified state, which exhibits a strong photoluminescence signal, may play an important role for the bistability.
 [DOI: 10.1063/1.1828603]

I. INTRODUCTION

Since the report by Faist *et al.*[1] on the realization and operation of quantum-cascade lasers (QCL's), various laser structures based on different designs and materials have been fabricated and characterized.[2] QCL's usually consist of a periodic repetition of two functional regions: an active region and an injector region. The population inversion is achieved by resonant coupling of the injector state with the upper laser level. This resonant coupling is expected to result in negative differential conductivity (NDC). As shown by Sirtori *et al.*,[3] NDC was experimentally observed in GaAs/AlAs diode structures, but not in GaAs/$Al_{0.33}Ga_{0.67}$As structures. Theoretical calculations of the transport properties of GaAs/(Al,Ga)As QCL's showed NDC only for structures with $Al_{0.45}Ga_{0.55}$As barriers.[4] In contrast to previous experimental and theoretical results, we found a pronounced NDC in undoped GaAs/$Al_{0.33}Ga_{0.67}$As quantum-cascade structures (QCS's) at a certain electric field strength denoted F_1. At the same time, the laser levels are populated at F_1.[5] An abrupt change of the intensity as well as the energy positions in the field-dependent photoluminescence (PL) spectra and the observation of current instabilities at F_1 show the complexity of the origin of NDC, which cannot be explained by a reduction of the coupling between the injector state and the upper laser level alone.

A detailed understanding of the origin of NDC in QCS's may contribute to an improvement of the laser characteristics such as efficiency, threshold current density, and population of laser levels. In particular, a comparison of the transport and population properties of QCS's containing $Al_{0.33}Ga_{0.67}$As and $Al_{0.45}Ga_{0.55}$As barriers is of great interest, since QCL's with $Al_{0.33}Ga_{0.67}$As barriers exhibit significantly higher threshold currents than lasers with $Al_{0.45}Ga_{0.55}$As barriers, which in part can be explained by the larger barrier height of the second system. In this paper, we focus on the analysis of NDC and current bistabilities in GaAs/$Al_{0.45}Ga_{0.55}$As QCS's using $I-V$ characteristics and interband PL spectroscopy as described in Ref. 6 for the GaAs/$Al_{0.33}Ga_{0.67}$As QCS's and compare the results with measurements on GaAs/$Al_{0.33}Ga_{0.67}$As QCS's.

II. EXPERIMENTAL DETAILS

The samples were grown by molecular-beam epitaxy on GaAs(100) substrates. While the GaAs/$Al_{0.33}Ga_{0.67}$As QCS's were based on the design by Sirtori *et al.*,[7] the GaAs/$Al_{0.45}Ga_{0.55}$As structures follow the layer sequence given by Page *et al.*[8] Our samples consist of 20 periods with undoped injectors. The cladding layers are replaced by 400-nm-thick n^+-GaAs contact layers in order to eliminate unintentional effects such as field inhomogeneities caused by the cladding layers. Using double-crystal x-ray diffraction measurements, the accuracy of the layer sequence was shown to lie within 2% of the nominal values with respect to the periodicity of the cascade and the average Al content. For one GaAs/$Al_{0.33}Ga_{0.67}$As QCS, we modified the first period of the cascade structure by removing the injection barrier so that it begins directly after the contact layer with a thinner barrier followed by the thickest quantum well instead of the injection barrier followed by the thinnest quantum well. This design was used to study the effect of the transition region between the contact layer and the cascade structure. For comparison, we also investigated a GaAs/$Al_{0.33}Ga_{0.67}$As double-quantum-well superlattice (DQWSL) with well widths of 5 and 4 nm as well as barrier widths of 10 and 14 nm. The transition region from the contact layer to the superlattice (GaAs contact, 10-nm $Al_{0.33}Ga_{0.67}$As barrier, 5 -nm GaAs quantum well) is similar to the one used in our unmodified QCS.

[a)]Electronic mail: htgrahn@pdi-berlin.de

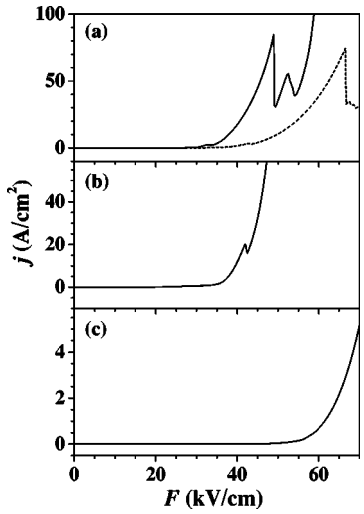

FIG. 1. $I-V$ characteristics (a) of the $GaAs/Al_{0.33}Ga_{0.67}As$ QCS with Ohmic (solid line) as well as Schottky (dashed line) contacts, (b) of the $GaAs/Al_{0.33}Ga_{0.67}As$ QCS with the modified first period, and (c) of the double-quantum-well superlattice.

For the transport and optical experiments, the samples were processed into mesa structures with Ohmic ring contacts allowing optical access from the top of the mesa. For the $GaAs/Al_{0.33}Ga_{0.67}As$ sample, we also fabricated Schottky contacts in order to determine the influence of the contacts on the transport properties. The diameter of the mesas was typically about 200 μm. The samples were mounted on a cold finger in a He-flow cryostat, and the temperature was set to 5 K. For the PL measurement, the samples were excited using a tunable Coherent Ti:sapphire laser (model 890) with an excitation energy of $E_{exc}=1.74$ eV, which is pumped by a Coherent Verdi V-5 (frequency-doubled $Nd:YVO_4$) laser. The PL signal was detected with a 1-m monochromator (Jobin–Yvon THR 1000) and a charge-coupled-device camera. For the transport measurement, the sample was connected to a current/voltage source (Hewlett–Packard, model 3245A) and a digital multimeter (Hewlett–Packard, model 3458A) in a two-terminal configuration.

III. RESULTS AND DISCUSSIONS

In order to determine the influence of the transition region between the metal contact and the GaAs n^+-contact layer as well as the effect of the injection characteristics from the GaAs contact layer into the cascade structure, we first describe the $I-V$ characteristics of the $GaAs/Al_{0.33}Ga_{0.67}As$ QCS's with different types of contacts (Ohmic versus Schottky) as well as unmodified and modified first period of the cascade. Figure 1(a) shows the $I-V$ characteristics of the $GaAs/Al_{0.33}Ga_{0.67}As$ QCS with the two different types of contacts. Both characteristics exhibit a pronounced NDC. However, the value of the critical field F_1 increases from 49 kV/cm for the sample with the Ohmic contact to 66 kV/cm for the sample with the Schottky contact. This increase in F_1 is clearly caused by the Schottky barrier at the contact, which results in an additional voltage drop and hence in a field inhomogeneity. This inhomogeneity is not taken into account when the (effective) field strength F is calculated by dividing the measured voltage by the thickness of the undoped layer system. Since the peak-to-valley ratio of the current is almost the same for both samples, we conclude that the pronounced NDC is determined by the cascade structure itself rather than by the contacts.

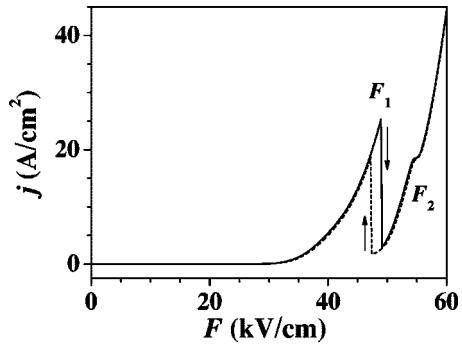

FIG. 2. I-V characteristics of the $GaAs/Al_{0.45}Ga_{0.55}As$ QCS for an up sweep (solid line) and a down sweep (dashed line). F_1 and F_2 denote the field strengths for NDC.

Figure 1(b) displays the $I-V$ characteristic for the $GaAs/Al_{0.33}Ga_{0.67}As$ QCS with the modified first period, i.e., with the enhanced injection of electrons from the top GaAs contact layer into the cascade. In comparison with the corresponding characteristic in Fig. 1(a) indicated by the solid line, the observed NDC is much less pronounced. At the same time, F_1 is decreased. In order to demonstrate that the transition region between the contact and the cascade alone is not the origin of the NDC, we present in Fig. 1(c) the $I-V$ characteristic of the DQWSL. In this sample, the transition region between the contact and the superlattice is very similar to the transition region in the original QCS, whose $I-V$ characteristic is shown in Fig. 1(a). The $I-V$ characteristic of the DQWSL does not show any pronounced NDC up to field strengths of 80 kV/cm. Therefore, we can rule out that the transition region between the contact and the cascade alone causes the NDC, although it seems to influence the detailed shape of the $I-V$ characteristics. We will return to this result when we discuss the influence of the carrier concentration on the NDC.

To determine the origin of the NDC, we will now compare the transport and optical properties of the $GaAs/Al_{0.33}Ga_{0.67}As$ QCS with the $GaAs/Al_{0.45}Ga_{0.55}As$ QCS. Figure 2 shows the $I-V$ characteristics of the $GaAs/Al_{0.45}Ga_{0.55}As$ QCS for an up sweep and a down sweep. A pronounced NDC appears at $F_1=49$ kV/cm, similar to the one already shown in Fig. 1(a) for the $GaAs/Al_{0.33}Ga_{0.67}As$ QCS and previously reported in Ref. 5. A hysteresis loop appears when the $I-V$ characteristics for the two sweeping directions are compared, indicating a bistability similar to the one observed for the $GaAs/Al_{0.33}Ga_{0.67}As$ QCS. However, in contrast to the $GaAs/Al_{0.33}Ga_{0.67}As$ QCS, a second, weaker NDC is observed at about $F_2=55$ kV/cm in the $GaAs/Al_{0.45}Ga_{0.55}As$ QCS, which may be attributed to the coupling of the injector with the upper laser level or to a coupling of the lower laser level with a state in the adjacent injector region. The appearance of the second NDC at F_2, which appears only in the $GaAs/Al_{0.45}Ga_{0.55}As$ QCS, agrees with the theoretical pre-

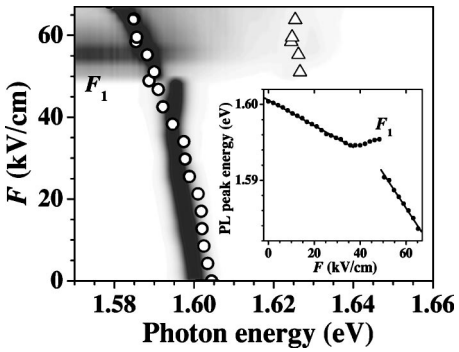

FIG. 3. Normalized, electric-field-dependent PL spectra of the conduction-band ground state and the lower laser level of the $GaAs/Al_{0.45}Ga_{0.55}As$ QCS in a gray-scale representation. For comparison, the calculated transition energies for the ground state (circles) and lower laser level (triangles) are added. The inset shows the dependence of the peak energy of the ground state on the electric field strength F.

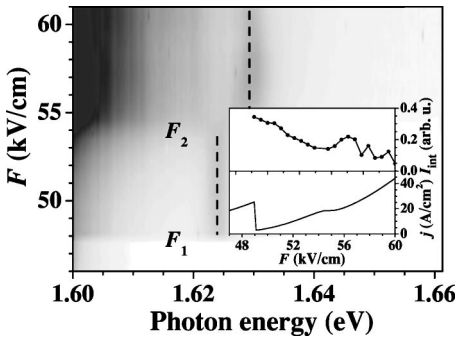

FIG. 5. Normalized PL spectrum in the vicinity of the lower laser level for the $GaAs/Al_{0.45}Ga_{0.55}As$ QCS as a function of F in a gray-scale representation. The inset shows the dependence of I_{int} of the PL line from the lower laser level and j on F. The vertical dashed lines indicate the different PL peak positions of the lower laser level for $F<F_2$ and $F>F_2$.

diction by Lee and Wacker[4] that NDC due to the anticrossing of the upper laser level with the injector state occurs only for the $GaAs/Al_{0.45}Ga_{0.55}As$ system.

Figure 3 shows the normalized PL spectra for the $GaAs/Al_{0.45}Ga_{0.55}As$ structure as a function of the electrical field strength F in a gray-scale representation. While for $F<49$ kV/cm the spectrum exhibits only a single line at about 1.60 eV, which is attributed to the direct transition between the ground states of the conduction and valence bands in the widest quantum well, the transition related to the lower laser level at about 1.63 eV appears abruptly at $F\approx 49$ kV/cm. This behavior is very similar to the one observed for the $GaAs/Al_{0.33}Ga_{0.67}As$ QCS.[6] The inset shows the dependence of the energy positions of the PL line due to the ground states in the widest quantum well on the applied electric field. For $F<35$ kV/cm, this PL line shifts with increasing field strength as a result of the quantum-confined Stark effect to lower energies. Between 35 and 49 kV/cm, the PL peak exhibits a small blueshift. At about 49 kV/cm, it jumps by about 5 meV to lower energies. For $F>49$ kV/cm, the PL energy shifts again continuously to lower energies. Note that, although the redshifts below 35 and above 49 kV/cm are both almost linear, their corresponding slopes are clearly different.

In Fig. 4, we compare the integrated PL intensity I_{int} of the ground-state interband transition as a function of F with the respective $I-V$ characteristic, both given in a semilogarithmic representation. Note that for this measurement we have chosen a rather small excitation power of about 1 μW in order to avoid any influence of the photoexcited carriers on the electron population distribution, i.e., the electron population distribution is completely determined by the electron transport within the QCS. While for $F<F_1$ the integrated PL intensity remains almost constant, it drastically decreases for $F>F_1$, i.e., the NDC is correlated with a strong quenching of the PL intensity of the ground-state interband transition. When the sample is excited with a higher excitation power of 10 μW, two PL peaks can be resolved for electric field strengths around F_1 (not shown here), which indicates that the PL lines for $F\ll F_1$ and $F\gg F_1$ are caused by two different transitions. While below F_1 the PL is related to the recombination of electrons and holes in the ground state of the conduction and valence bands, respectively, of the widest quantum well, the recombination for $F>F_1$ seems to be related to electrons in a conduction-band state of the adjacent injector with holes of the same valence-band ground state in the widest well. The different slopes of the redshift of the PL lines below 35 and above 49 kV/cm are also an indication for the different origin of the respective PL lines. The blueshift between 35 and 49 kV/cm may be caused by an accumulation of space charge in the active region, which would partially screen the external electric field. The switching behavior of the PL intensity may be an indication for a carrier redistribution process within the QCS at the critical field strength.

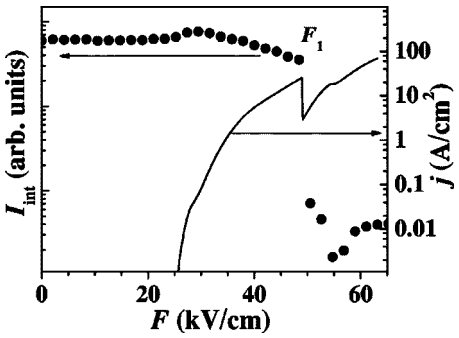

FIG. 4. Integrated PL intensity I_{int} of the interband PL transition lowest in energy and current density j as a function of F for the $GaAs/Al_{0.45}Ga_{0.55}As$ QCS. At F_1, an abrupt decrease of the PL intensity is observed.

As for the $GaAs/Al_{0.33}Ga_{0.67}As$ QCS,[6] the abrupt decrease of the integrated PL intensity as shown in Fig. 4 is connected with the population of the laser levels. Figure 5 displays the field dependence of the PL spectra for the PL line due to the lower laser level for electric fields between 46 and 61 kV/cm in a gray-scale representation. Below F_1, no PL signal from the lower laser level is detected. At $F_2=55$ kV/cm, the appearance of the second NDC is correlated with a blueshift of the PL line of the lower laser level by about 5 meV. This blueshift may be due to a charge redistribution in the active region, which is triggered by the coupling of the upper laser level with the injector state. The inset depicts the field dependence of I_{int} of the lower laser level in

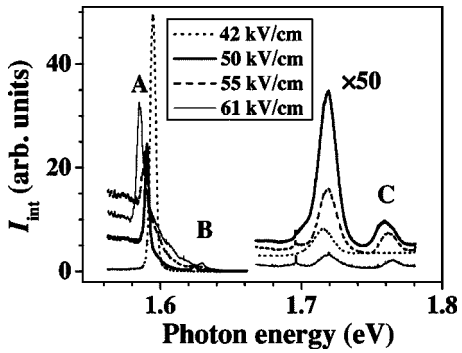

FIG. 6. PL spectra of the $GaAs/Al_{0.45}Ga_{0.55}As$ QCS recorded for different electric field strengths as indicated showing the ground-state transition (A), the lower laser level (B), and the upper laser level (C). The PL spectra at higher energies (1.67–1.78 eV) have been multiplied by a factor of 50 and shifted vertically for clarity.

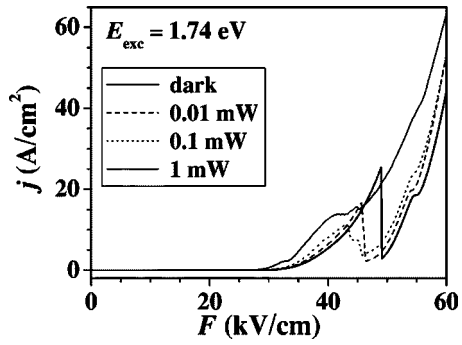

FIG. 7. $I-V$ characteristics under illumination for different excitation powers at an excitation energy of 1.74 eV for the $GaAs/Al_{0.45}Ga_{0.55}As$ QCS.

comparison with the $I-V$ characteristics. The integrated PL signal exhibits a small maximum near F_2. Since the field strength for the abrupt energy shift of the PL line of the lower laser level in Fig. 5 depends on the carrier density, this switching cannot be related to an anticrossing of the lower laser level with a state in the adjacent injector. While for the $GaAs/Al_{0.45}Ga_{0.55}As$ QCS's F_1 is significantly smaller than F_2, both field strengths may coincide for the $GaAs/Al_{0.33}Ga_{0.67}As$ QCS's as shown by the anticrossing behavior in Ref. 9. The resonant coupling through the injector barrier seems to be weaker for the $GaAs/Al_{0.45}Ga_{0.55}As$ QCS as compared with the $GaAs/Al_{0.33}Ga_{0.67}As$ QCS. Therefore, we cannot resolve a splitting of the PL line attributed to the upper laser level and consequently an anticrossing of the upper laser level with the injector level.

Figure 6 shows the spectra of the three PL lines due to the transitions of electrons in the ground state (A) as well as in the lower (B) and upper laser level (C) with holes in the ground state of the widest quantum well for the $GaAs/Al_{0.45}Ga_{0.55}As$ QCS for several electric field strengths. Note that in order to detect the upper laser level the excitation power had to be increased to 10 mW. At about 50 kV/cm, the energy difference between the upper and the lower laser level is about 130 meV, which agrees with the lasing energy observed by Page *et al.*[8] In contrast with the $GaAs/Al_{0.33}Ga_{0.67}As$ structures, a fourth, very strong PL peak appears at about 1.72 eV, which will be discussed below.

We believe that the strong NDC at F_1, which exhibits a bistable behavior, is related to a field inhomogeneity generated by a charge accumulation in the active region, while the NDC at F_2 without any bistability is merely caused by resonant coupling of the upper laser level with the injector level. Below F_1, some of the electrons, which are injected from the contact, accumulate inside the active region. If the field screening caused by these carriers is sufficiently large, it can substantially modify the conduction-band-edge profile and induce a significant redistribution of the electron population. In order to study the dependence of the NDC on the carrier density, we measured the $I-V$ characteristics under illumination for several different excitation intensities resulting in different carrier densities, which are shown in Fig. 7. For weak excitation (0.01 mW), F_1 shifts in comparison with the $I-V$ characteristic recorded without any illumination to lower field strengths. For strong excitation (1 mW), the NDC disappears. Instead, a plateaulike structure is observed as already reported for $GaAs/Al_{0.33}Ga_{0.67}As$ QCS's by Ohtsuka *et al.*[10] In addition, the peak-to-valley ratio of the current decreases with increasing carrier density. The $I-V$ characteristic of the QCS with a modified first period also shows a shift of the NDC to lower-field strengths as well as a decrease of the peak-to-valley ratio. Therefore, we conclude that the stronger coupling of the first period of the cascade to the GaAs contact layer changes the $I-V$ characteristic and possibly increases the density of injected electrons. In contrast to this behavior, the NDC at F_2 is almost independent of carrier density.

The mechanisms, which lead to the bistable NDC, and their correlation with the laser level population may also be responsible for the additional strong PL line at 1.72 eV shown in Fig. 6, which appears between the lower and upper laser levels. We have not been able to identify the origin of this peak using calculations of the subband energies. In addition, the energy position of this peak remains almost constant with increasing electric field. Therefore, this peak may be attributed to a barrier or interface state rather than to a subband state of a QW in the injector region. The maximum PL intensity of this peak is observed at F_1. This indicates that this state may induce a transport channel for the electrons within the (Al,Ga)As barrier and can lead to a modification of the carrier distribution.

IV. SUMMARY AND CONCLUSIONS

We have investigated the appearance of NDC in undoped GaAs/(Al,Ga)As QCS's with different Al contents. While for $GaAs/Al_{0.45}Ga_{0.55}As$ as well as $GaAs/Al_{0.33}Ga_{0.67}As$ QCS's a pronounced bistable NDC is observed at F_1, a second, weaker NDC at $F_2 > F_1$ without any bistability appears only in $GaAs/Al_{0.45}Ga_{0.55}As$ QCS's. The field strength of the strong NDC at F_1 can be changed by a variation of the carrier density and by different types of contacts. Although the NDC at F_1 is accompanied by a strong increase of the population of the laser levels and an abrupt decrease of the population of the ground state, it cannot be explained by the resonant coupling between the injector and upper laser level. We rather attribute the weaker NDC

at F_2 to this resonant coupling, because it agrees with the theoretical prediction that it should only be present in $GaAs/Al_{0.45}Ga_{0.55}As$ QCS's. Although at this point in time we cannot give a complete model for the strong NDC, we believe that it is caused by an interplay of resonant coupling effects within the injector with field inhomogeneities due to charge accumulation. Even the influence of an additional state, which has not yet been identified, but manifests itself through an additional PL line with a maximum intensity at F_1, cannot be excluded as a possible source for NDC. For the $GaAs/Al_{0.33}Ga_{0.67}As$ QCS's, both NDC regions may appear at the same field strength so that in this case the NDC without any bistability due to the resonant coupling between the injector and upper laser level is masked.

ACKNOWLEDGMENT

This work was supported in part by the Deutsche Forschungsgemeinschaft within the framework of the Forschergruppe 394.

[1] J. Faist, F. Capasso, D. L. Sivco, C. Sirtori, A. L. Hutchinson, and A. Y. Cho, Science **264**, 553 (1994).
[2] C. Gmachl, F. Capasso, D. L. Sivco, and A. Y. Cho, Rep. Prog. Phys. **64**, 1533 (2001), and references therein.
[3] C. Sirtori, H. Page, C. Becker, and V. Ortiz, IEEE J. Quantum Electron. **38**, 547 (2002).
[4] S. C. Lee and A. Wacker, Phys. Rev. B **66**, 245314 (2002).
[5] L. Schrottke, R. Hey, H. Kostial, T. Ohtsuka, and H. T. Grahn, Physica E (Amsterdam) **21**, 852 (2004).
[6] L. Schrottke, T. Ohtsuka, R. Hey, H. Kostial, and H. T. Grahn, Semicond. Sci. Technol. **19**, 421 (2004).
[7] C. Sirtori, P. Kruck, S. Barbieri, P. Collot, J. Nagle, M. Beck, J. Faist, and U. Oesterle, Appl. Phys. Lett. **73**, 3486 (1998).
[8] H. Page, C. Becker, A. Robertson, G. Glastre, V. Ortiz, and C. Sirtori, Appl. Phys. Lett. **78**, 3529 (2001).
[9] L. Schrottke, R. Hey, and H. T. Grahn, Appl. Phys. Lett. **84**, 4535 (2004).
[10] T. Ohtsuka, L. Schrottke, R. Hey, H. Kostial, and H. T. Grahn, J. Appl. Phys. **94**, 2192 (2003).